13th World Conference on Earthquake Engineering
Vancouver, B.C., Canada
August 1-6, 2004
Paper No. 18

Cyclic Test on Composite Wall-Frame Subassemblage

Kenji Sakino [1], Toko Hitaka[2] and Yutaka Ueda[3]

SUMMARY

This paper reports on a research project aimed at investigating a dual system composed of moment-resisting open frames and new type of wall systems utilizing concrete filled steel tubular (CFT) columns. This proposed wall system is similar to a coupled wall system in appearance. The main differences between them are followings; (1) two cantilever walls coupled by coupling devices have horizontal clearances whose height is nearly equal to edge column depth at the top and the bottom of walls, hence, each wall is connected to a foundation beam and a top beam only through edge columns which are concrete filled steel tubular columns or reinforced concrete columns confined in square steel tube, (2) the reinforced coupling girders of the coupled wall system are replaced by steel shape girders placed at the top floor level and at the bottom floor level, or only diaphragm system in other floor levels. The wall systems proposed in this paper are expected to act as hysteretic dampers since the steel coupling devices are designed so as to yield at a small story drift and to absorb large energy. This paper describes the experimentally obtained seismic performances of the proposed wall systems which were obtained by the tests on four 1/4-scale model frame and wall specimens. The experimental results show that the specimens to be designed appropriately behave in a ductile manner and have very large energy absorption capacity available even in small story drift.

INTRODUCTION

In many reinforced concrete buildings, reinforced concrete frames and structural walls appear together. When lateral force resistance is provided by the combined contribution of frames and structural walls, it is customary to refer to them as a wall fame system, a dual system or a hybrid system. The Japanese term related to this type of system can be translated literally as wall frame system.

Figure 1(a) shows in plan the somewhat idealized disposition of frames and walls in 12-story symmetrical examples structure. The Japanese “Design Guidelines for Earthquake Resistant Reinforced Concrete Buildings Based on Ultimate Strength Concept” (Architectural Institute of Japan (AIJ), 1997, referred to as AIJ Guidelines hereafter) have prescribed a design method applicable to the wall frame system shown in Figure 1. The design procedure prescribed in AIJ Guidelines is similar to “Capacity Design Procedure” in New Zealand in many respects. Yield or failure mechanisms of the structural walls shown in Figure

[1] Professor, Faculty of Human-Environment Studies, Kyushu University, Japan
[2] Reserch Associate, Faculty of Human-Environment Studies, Kyushu University, Japan
[3] Student, Faculty of Human-Environment Studies, Kyushu University, Japan

1(b) can be roughly classified into three types, which are called as a shear failure, a flexural yield mechanism and a rotation mechanism as shown in Figure 2(a) (b) and (c), respectively. The AIJ Guidelines prescribed that the shear failure of structural walls be avoided since it results in a soft story collapse mechanism of buildings. The AIJ Guidelines also prescribed that the principal sauce of energy dissipation in a laterally loaded structural wall must be the yielding of the flexural reinforcement in the plastic hinge regions, normally at the base of the wall, as shown in Figure 2(b). In order to expect the flexural yield mechanism of walls, however, a foundation system of the building should be designed to resist a large tension force induced in the tension edge column of the wall, which is inevitable for the wall to yield in flexure. In order to avoid such a heavy foundation system, the rotation mechanism of the wall, which introduces the loss of principal sauce of energy dissipation, must be reluctantly accepted. Moreover, the flexural yield mechanism is not necessarily to be desirable mechanism because of following reasons.

(1) The volumes of plastic hinge regions developed in structural walls are expected to be so large that many remarkable cracking of concrete would occur, which is not desirable from a view point of performance based design.

(2) It is difficult to prevent a web crushing failure of walls yielded in flexure and subjected to cyclic loading with large ductility demand (Bertero et al. 1977).

(3) An interaction between frames and structural walls with plastic hinges at the bottom is too complicated to be analytically considered in practical design since the rotation of the wall plastic hinge about a point close to the compression edge column at the base could introduce three-dimensional effects into wall frame structures.

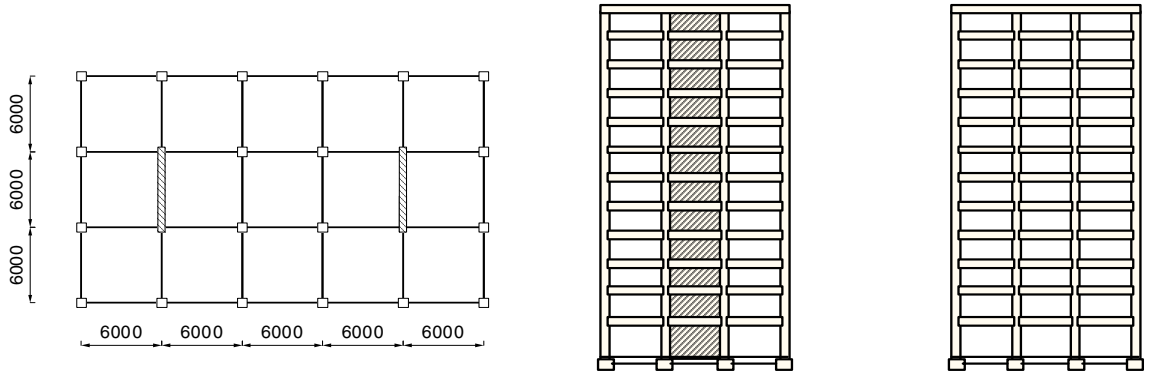

(a) Plan (b) Structural wall (c) Frame

Figure 1 Typical wall frame system.

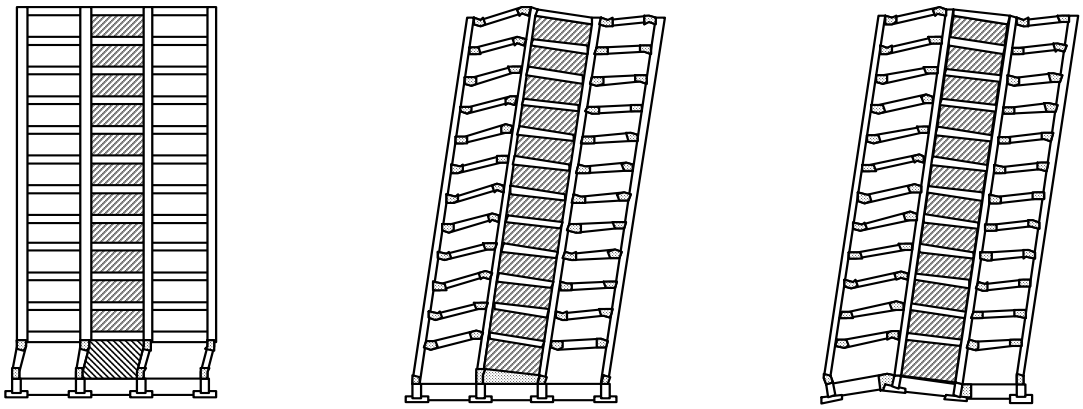

(a) Shear failure (b) Flexural yield mechanism (c) Rotation mechanism

Figure 2 Collapse mechanisms of structural wall

If the flexural yield mechanism shown in Figure 2(b) is not necessarily desirable, we should come up with the alternative desirable mechanism of structural walls. This will be discussed in the following sections

OVERTURNING COLLAPSE MECHANISM WALL

The alternative desirable mechanism of structural walls proposed in this paper is shown in Figure 3. This structural wall is named as overturning collapse mechanism wall (OTC wall). A kinematically admissible complete mechanism of the wall shown in Figure 3 is developed when four plastic hinges formed in edge columns at the top and bottom of the wall and the shear yielding of the two coupling girders installed in the wall are fully developed. The most important conception adopted in this wall is to provide horizontal clearances between wall panel and foundation and roof beams with a height nearly equal to the depth of the edge columns. These clearances enable the wall system to develop the collapse mechanism without any damages in the wall panels. Moreover, these clearances make a different between OTC walls and coupled structural walls (Paulay et al. 1992). Figure 4 shows different types of OTC walls which have horizontal clearances in common, but have different types of vertical slot or openings. The characteristics and merits of the OTC walls are itemized as followings.

(1) Plastic deformations or damages of the wall during a major earthquake could be limited in four plastic hinges in edge columns and coupling girders or vertical steel bars provided in horizontal clearances (see Figure 4b), the rest of the wall including concrete wall panels in the first story can be designed to stay in elastic regions. Hence, the analytical model for the wall applicable to both of static and dynamic analysis can be simple and reliable.

(2) Initial yielding of coupling girders (or vertical steel bars) occurs at an early stage of lateral loading in small interstory drift level. If the coupling girders (or vertical steel bars) are designed to be able to dissipate large amounts of energy input without collapsing under extreme loading condition during major earthquakes, coupling girders can take a role of hysteretic dampers during earthquakes. Such a design can be easily achieved by using H-shaped steels as coupling girders or buckling restrained steel bars.

(3) A deformation pattern of an OTC wall subjected to lateral load is similar to that of a frame; hence the OTC wall does not bring a complicated three-dimensional effect into wall frame structures.

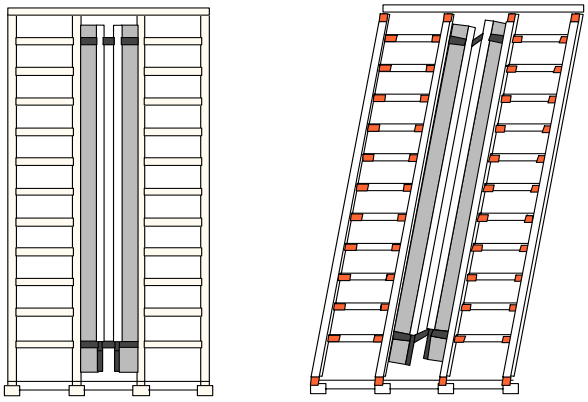

Figure 3 Overturning collapse mechanism wall (OTCwall).

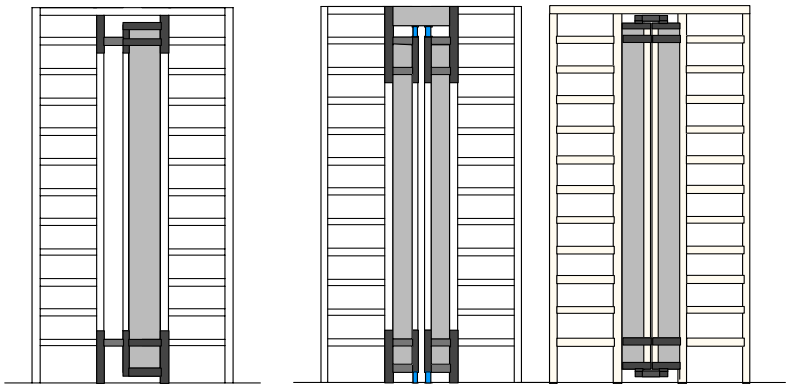

(a) Side opening type (b) Vertical slot type

Figure 4 Other types of OTC walls.

(4) A tension force induced in the bottom edge column in tension side at the ultimate state can be determined from gravity load, capacity of the beams framing into the wall system and capacities of coupling steel girders. Hence, the tension force in the edge columns can be controlled independently of a tension capacity of the edge column.

Needless to say, OTC walls as well as properly detailed structural walls provided a nearly optimum means of fulfilling basic criteria that the designers will aim to satisfy, i.e. stiffness, strength, and ductility. Unfortunately, the view that structural walls are inherently brittle is still hold in many countries as consequence of shear failure in poorly detailed walls as well as squat structural walls. For this reason, Japanese Building Law and AIJ Guidelines penalize wall frame structures, i.e. they require buildings with structural walls to be designed for lower ductility factors or larger capacity demands or larger earthquake forces than frames. A major aim of our research on OTC walls is to show that buildings with OTC walls are rather superior to ductile moment resisting space frame buildings. It is emphasized that OTC walls are not reinforced concrete structural walls, but composite structural walls in which steel is used to dissipate energy input or to confine concrete, on the other hand, concrete is used to secure the stiffness.

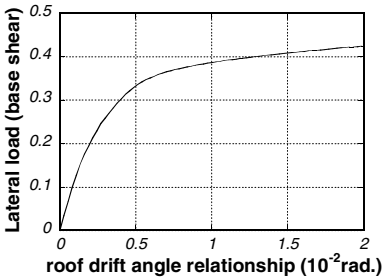

Figure 5 Lateral load (base shear) versus roof drift angle relationships.

In order to plan an experimental program on OTC walls and to evaluate experimental results, the 12-story building shown in Figure 1 was tentatively designed and analytically investigated (Hitaka et al. 2003). The reinforced concrete structural walls shown in Figure 1(b) was replaced by the OTC walls shown in Figure 3, and tubed RC columns (Tomii et al. 1987), which were RC columns confined in steel tubes instead of ordinal hoops, were used as the columns in frames. Main analytical results are shown in Figures 5 –7. A brief description of analytical method will be described later. Figure 5 shows the static behavior of the building obtained by a non-linear pushover analysis. Figure 6 shows interstory drift envelopes of the building obtained by dynamic inelastic time-history analysis under the El Centro 1940 NS which was scaled such that the peak ground velocity (PGV) will be equal to 0.25, 0.50, 0.75 and 1.00 m/sec. Figure 7 shows the maximum shear force carried by one OTC wall system. The results are of the analysis with the three kinds of earthquake waves scaled to 1.0 m/sec. The pushover analysis result at the roof drift angle of 1/100 is compared with the dynamic analysis results. As shown in Figure 6, a seismic performance of the building with OTC walls is excellent because of its small interstory drift response to the major earthquake, which implies that an overturning capacity of this building could be reduced. The results shown in Figure 7 will be discussed along with experimental results in following sections.

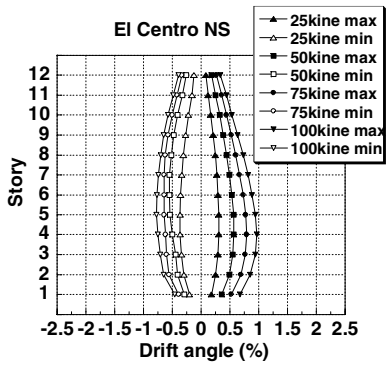

Figure 6 Maximum interstory drift envelope responses to El Centro NS Earthquake.

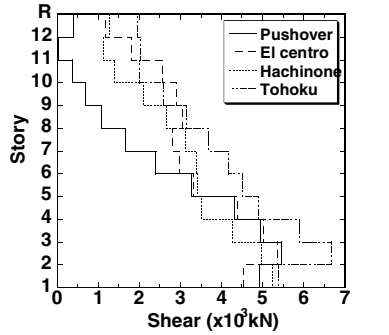

Figure 7 Maximum shear forces carried by OTC wall system.

EXPERIMENTAL PROGRAMS

TEST SPECIMENS

The matter of major interest in the experimental study was to investigate the collapse mechanisms of different types of OTC walls as well as frame with the tubed RC columns. Seven 1-bay, 1-span model subassemblage specimens isolated from the 12-story building shown in Figure 1 (referred to as the prototype building hereafter) were constructed and tested. The seven specimens were scaled to 1/4 in order to utilize the available test facility. Two of them were an open frame model, and the others were structural wall models. The frame specimens were tested to compare the mechanical behavior of the frames and walls. The five types of wall specimens are corresponding to three types of OTC walls shown in Figures 3 and 4. The dimensions and detailing of the specimens basically follow the dimensions and detailing of the prototype building and are shown in Figure 8. However some detailing is different from the prototype as described below for each specimen. The properties of each specimen and materials are shown in Table 1.

Table 1 Properties of materials for each specimen

		σ_y (N/mm^2)	σ_u (N/mm^2)	$_c\sigma_B$ (N/mm^2)
STF, RCF, WCOT, WCO	H-175x175x7.5x11	287	455	
	Steel Tube(□-175x175x6)	338	451	
	D10 Steel Bar	354	496	
	D13 Steel Bar	338	500	
	Columns, Beams			40
	Wall Panel			108
WSO	H-175x175x7.5x11	327	485	
	Steel Tube(□-175x175x6)	411	480	
	Columns			41
	Wall Panel			113
WVD	Vertical Damper	335	499	
	Steel Tube(□-175x175x6)	411	480	
WHD	H-175x175x7.5x11	334	489	
	Steel Tube(□-175x175x6)	411	480	
WVD, WHD	Columns			38
	Wall Panel			87

Frame Specimen STF (Figure 8(a)): This specimen was fabricat ed by the tubed RC columns and a steel beam with H shape section, and designed to fail in a mechanism where plastic hinges were developed at the bottom and top of the columns. Eight deformed bars with nominal diameter of 9.5mm (D10 bar) were used as longitudinal bars.

Frame Specimen RCF (Figure 8(b)): This specimen was fabricated by the tubed RC columns and a reinforced concrete beam, and designed to fail in a mechanism where plastic hinge s were developed at the bottom of the columns and both ends of the RC beam. Six D10 bars were used as longitudinal bars of

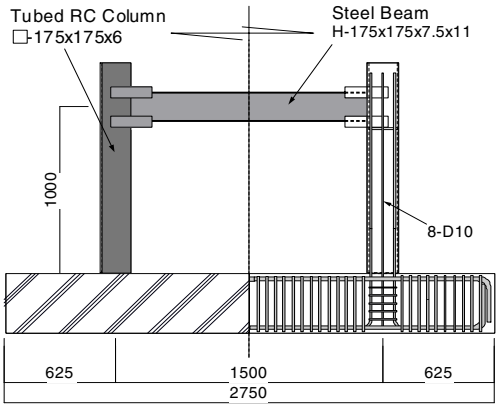

(a) STF Specimen

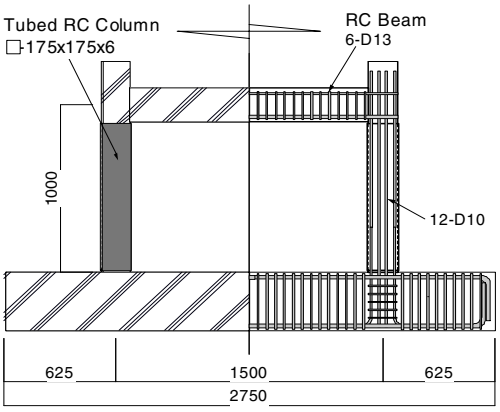

(b) RCF Specimen

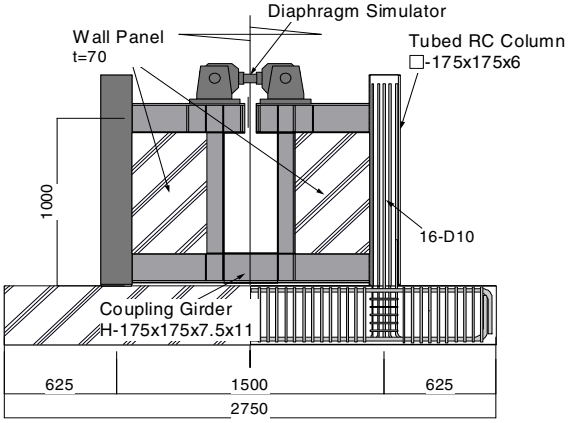

(c) WCOT Specimen

Figure 8 Details of test specimens.

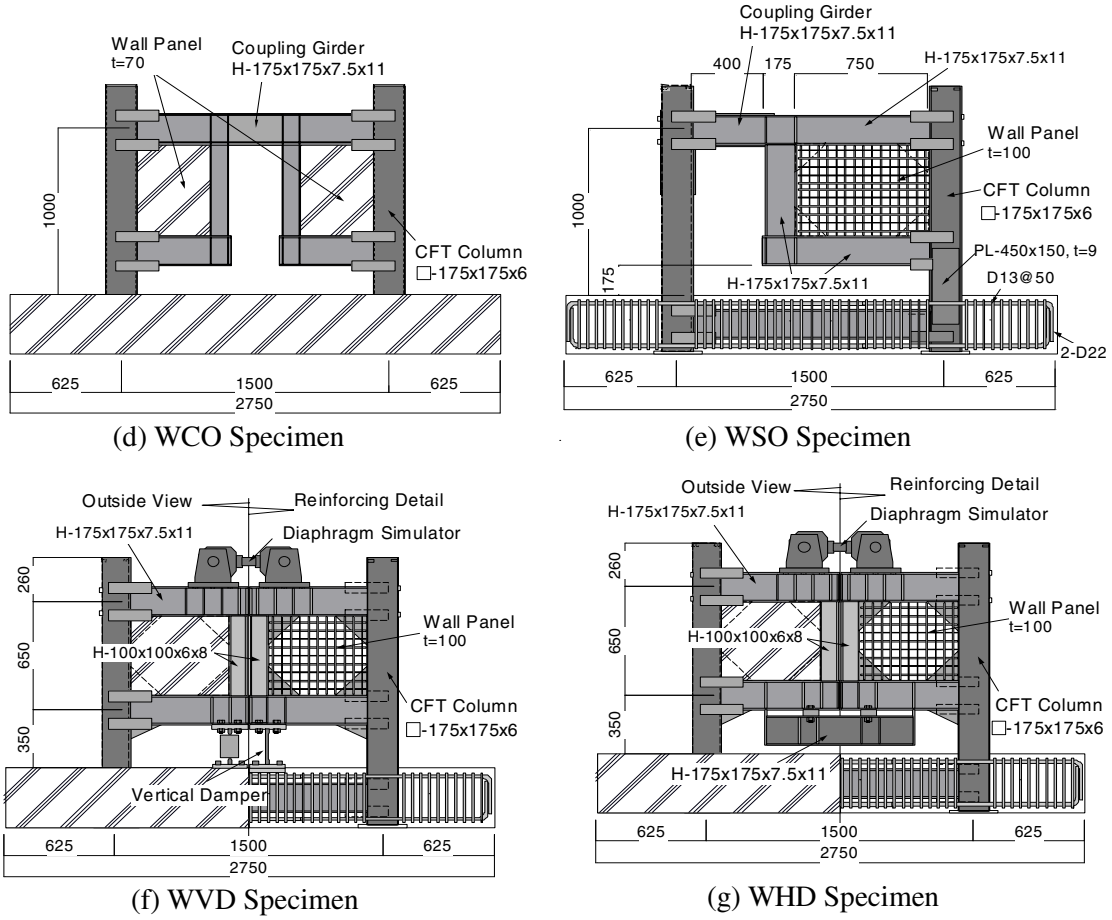

Figure 8 Details of test specimens (Continue).

beam, and twelve D10 bars were used as longitudinal bars of columns.

Wall Specimen WCOT (Figure 8(c)): This wall specimen models the OTC wall with a central opening for a doorway shown in Figure 3. The coupling gird ers of the specimen is designed to have a shear cap acity which is nearly equal to the sum of the top (12th floor) and the bottom (2nd floor) coupling girders. Then the specimen has the overturning moment capacity nearly equal to that of the structural wall in the prototype building. The edge columns were made by tubed RC columns in which sixteen D10 bars were used as longitudin al bars. The amount of longitudinal bars was 4.3%. The composite wall panels were designed using high strength plain concrete with 70mm thickness and steel plate of 3.5mm thickness with stiffeners in order to carry the maximum shear force applied to the wall panel which was expected to be much larger than that of the prototype building because the concentrated lateral load was applied at the second floor level as described later. The steel plate panel of 3.5mm thickness with stiffeners was attached to surrounding steel frame by welding only one side of wall panel which enabled concrete casting. The detail of the composite wall panel is shown in Figure 9. A horizontal clearance of 10mm between the foundation beam and the lower face of the steel beam in boundary frame of the wall panel was provided to prevent the tubed RC columns from a punching shear failure (see Figure 9). In this type of the OTC wall, two walls should be weakly coupled by diaphragm system designed by a special manner. As shown in Figure 8(c), two walls are connected by a special device named diaphragm simulator which can transfer only axial force. The diaphragm simulator was designed as a load cell in order to estimate shear forces resisted by each wall through the test.

Wall Specimen WCO (Figure 8(d)): This wall specimen also models the OTC wall with a central opening for a doorway shown in Figure 3. The tubed columns in WCOT specimen was replaced by CFT columns. The detail of composite wall panels was similar to that of WCOT specimen. It is noteworthy that the steel plates for wall panels were used only for these two specimens. Reinforced concrete wall panels of the other three wall specimens, which were designed and fabricated after the test of these two specimens, were fabricated without steel plate panels because it was concluded that the steel plate panels were not necessary as far as a shear capacity of the wall panels were concerned.

Wall Specimen WSO (Figure 8(e)): This specimen models the OTC wall with a side opening for a doorway shown in Figure 4(a). The coupling girder on the specimen is designed by using the same steel shape as that of Specimen WCO. The wall panel was reinforced concrete panel with high strength concrete. The width of the opening was slightly wider than that of the Specimen WCO, which required the cover plates for flanges of coupling girder to prevent a flexural failure of the girder. The isolated CFT columns, which was the other side the w all panel, was reinforced by welding the steel cover plate to the flanges of the steel tube in a potential plastic hinge region adjacent to beam to column connection. The bottom of the CFT edge column of the wall was reinforced by welding the steel cover plates to the webs of the steel tube in a potential plastic hinge region.

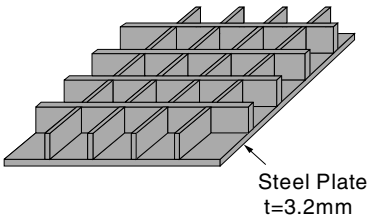

Figure 9 Detail of composite wall panel in WCO and WCOT specimens.

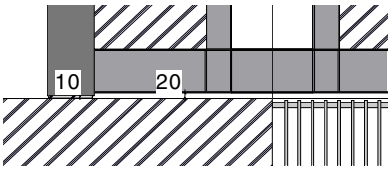

Figure 10 Detail of bottom part of WCOT specimen.

Wall Specimen WVD (Figure 8(f)): This specimen models the OTC wall with a vertical slot shown in Figure 4(b). In this type of the OTC wall, roles of the couplings girders are taken by buckling restrained steel bars installed in the clearance between wall panel and foundation beam. Details of the steel bar called as a vertical damper is shown in Figure 11(a). The diaphragm simulator was installed for this specimen in the same manner as for WCOT specimen.

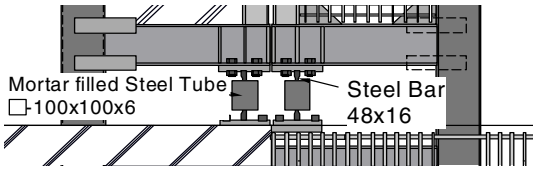

(a) Vertical damper for WVD specimen

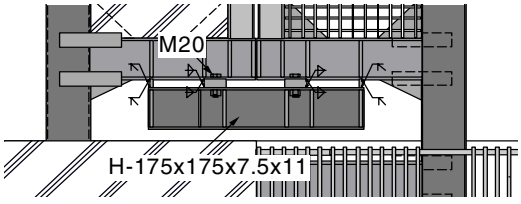

(b) Horizontal damper for WHD specimen

Figure 11 Details of dampers.

Wall Specimen WHD (Figure 8(g)): The one of the features of OTC wall is that the energy absorption devices such as coupling girder or vertical damper can be easily repaired or replaced by new one after a severe earthquake event. This sp ecimen was fabricated by replacing the damaged vertical dampers of WVD specimen after the test with the coupling girder shown in Figure 11(b) which was the H-shaped beam with the same dimension of that in WCO and WSO specimens.

EXPERIMENTAL APPARATUS AND PROCEDURE

A loading method is schematically shown in Figure 12. The vertical load corresponding to gravity load in the inner columns of prototype building at the first story, which was 265 kN per column, was applied to the specimen at first, and kept constant during the cyclic lateral loading test. The horizontal loads were

applied to the specimen in a manner of pushing in both directions as shown in Figure 13, which introduced the compression axial force into the beam. It is noteworthy that the horizontal loads were always applied at the second floor level through the test. This means that an inflection point of the wall specimens is fixed at the second floor level. However, an actual inflection point of the structural walls in the prototype building might fluctuate during horizontal loadings especially in the case of dynamic loadings, and might be much higher than the second floor level. Therefore, the shear forces induced in the wall specimens will be much larger than those of the walls in the prototype building at the ultimate state where the collapse mechanism of the building is fully developed. In other words, the effects of shear force on the mechanical behavior of wall specimens are amplified in the tests using the test set-up schematically shown in Figure 12. The displacements, δ_1, δ_2 and δ_3 shown in Figure 13 were measured to determine story drift angles and member deformation angles of coupling girders. The loading pattern was a cyclic type with alternating drift reversals. The peak drifts were increased stepwise from 0.002h, where h was the story height, until 0.02h with incremental drift of 0.002h or 0.003h after three successive cycles at each drift level as shown in Figure 14.

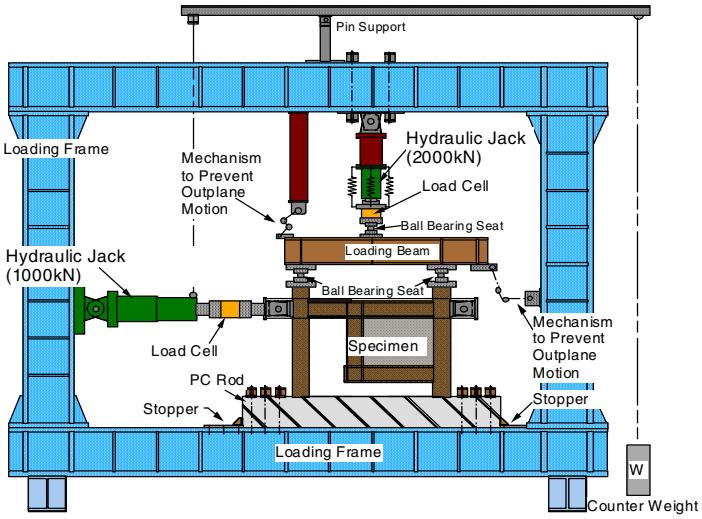

Figure 12 Loading set-up.

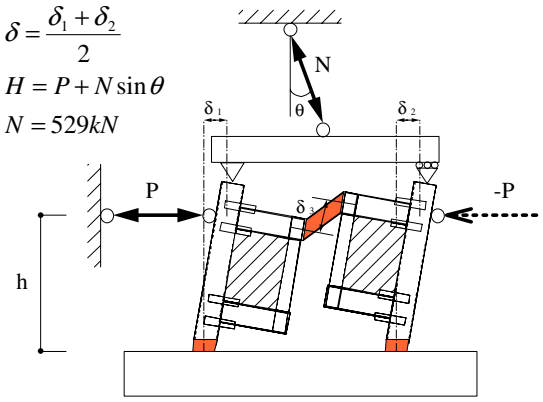

Figure 13 Loading method and displacements measured.

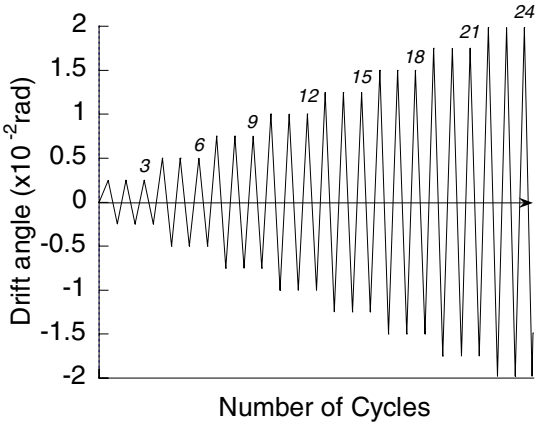

Figure 14 Loading program.

EXPERIMENTAL RESULTS AND DISCUSSION

COLLAPSE MECHANISMS

The cyclic loading tests up to the story drift of 0.02h showed that the expected collapse mechanism was realized in the test of each specimen except for WVD specimen. Undesirable failures in plastic regions, such as cracks in welding portion, local buckling of the steel tube in the CFT columns and H-shaped steel coupling girders were not observed in any specimens. In RCF specimen, crushing of concrete in the RC beam plastic hinges was slightly observed. In wall specimens, only a few fine diagonal cracks were

observed in concrete of wall panels. In WCOT specimen, a sliding shear slip at the bottoms of tubed RC columns was observed at the final state where the story drift was larger than 0.015h. In WVD specimen, tension fractures of the buckling restrained steel bars (vertical dampers) occurred just after the three successive cyclic loadings at story drift level of 0.015h. One of the reasons for the premature rapture of steel bars was plastic hinging developed at both ends of the steel bars where the steel bars were not covered by buckling restraining device. The large rotation of the plastic hinges was considered to reduce the elongation capacity of the steel bars. It was concluded that all the specimens except for WCOT and WVD specimens behaved in an excellent manner from view points of the performance-based design philosophy, and it was also concluded that WVD specimen was successfully rehabilitated by replacing the energy absorption device after a severe earthquake. It should be emphasized that indications of any kinds of shear failure were not observed in the bottom of the CFT columns of wall specimens even though these wall specimens were subjected to shear forces much larger than those estimated by the static pushover and dynamic response analyses of the prototype building and shown in Figure 7. It could be said that the sliding shear slip at the bottoms of the tubed RC columns of WCOT specimen wouldn't occur under the loading condition expected from the dynamic response analysis of the prototype building. It can be also said that the tubed RC columns can be used as the edge columns at the top of the OTC wall. Figure 15 shows the remarkable features of test specimens after the tests. Figure 15(a) shows an example of the overturning collapse mechanism observed in WSO specimen at final state where the story drift reached to 0.06h. Figure 15(b) shows a close up photo of the fractured steel bar in WVD specimen.

(a) WSO specimen (Story drift = 0.06h)

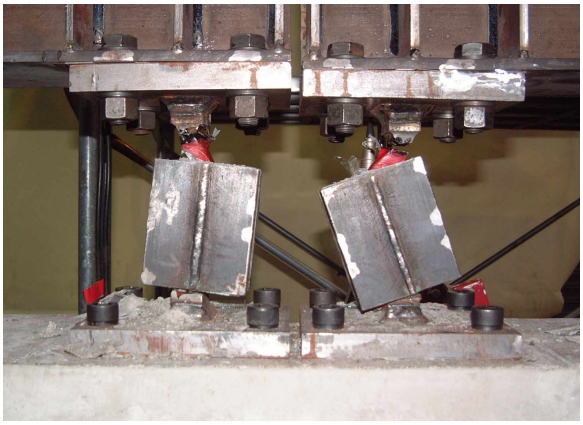

(b) Fracture of vertical damper in WVD specimen

Figure 15 Test specimens after tests

RELATIONSHIPS BETWEEN LATERAL LOAD AND INTERSTORY DRIFT

Figure 16 shows relations between the lateral load and the story drift of seven specimens. As shown in Figure 16, lateral load carrying capacity of wall specimens are 5 to 8times of the frame specimens. Lateral stiffness and energy absorption capacity of WCO specimen are larger than those of WSO, WVD or WHD specimens. The main reason for this phenomenon is considered that the wall panels of WCO specimen w ere stiffened by the steel plate panels welded to the boundary steel frames, and then the shear deformations of wall panels were negligible. In the cases of WSO, WVD and WHD specimens, shear deformations of wall panels cannot be negligible, because the concrete in wall panel is not effective in tension. It should be noted, however, that the effects of shear force on the mechanical behavior of wall specimens are amplified due to the lateral loading method adopted in this tests as mentioned in preceding section. Therefore, the OTC walls shown in Figure 4 can be more effectiv e hysteretic dampers tha n expected from test res ult s shown in Figure 16(e), (f) or (g). A pinching effect is observed in the hystere

tic curves of WCOT specimen at the story drift amplitude larger than 0.015h due to the sliding shear slip at the bottoms of the tubed RC columns described in preceding section. An abrupt deterioration of overturning moment capacity at story dr ift of 0.018h is observed in WVD specimen, which is resulted from ruptures of both steel bars (vertical dampers), described in preceding section. Figur e 16 (c)-(g) shows that all the wall specimens have enough shear capacity compare to the demand shown by the linked li ne that was obtained from Figure 7. The wall specimens did not fail due to shear but failed in overturning collapse mechanism. This means that the potential shear capacities of the wall specimens were larger than the experimental lateral load capacities.

Dotted lines in Figure 16 show the overturning moment capacity of wall specimens calculated by an

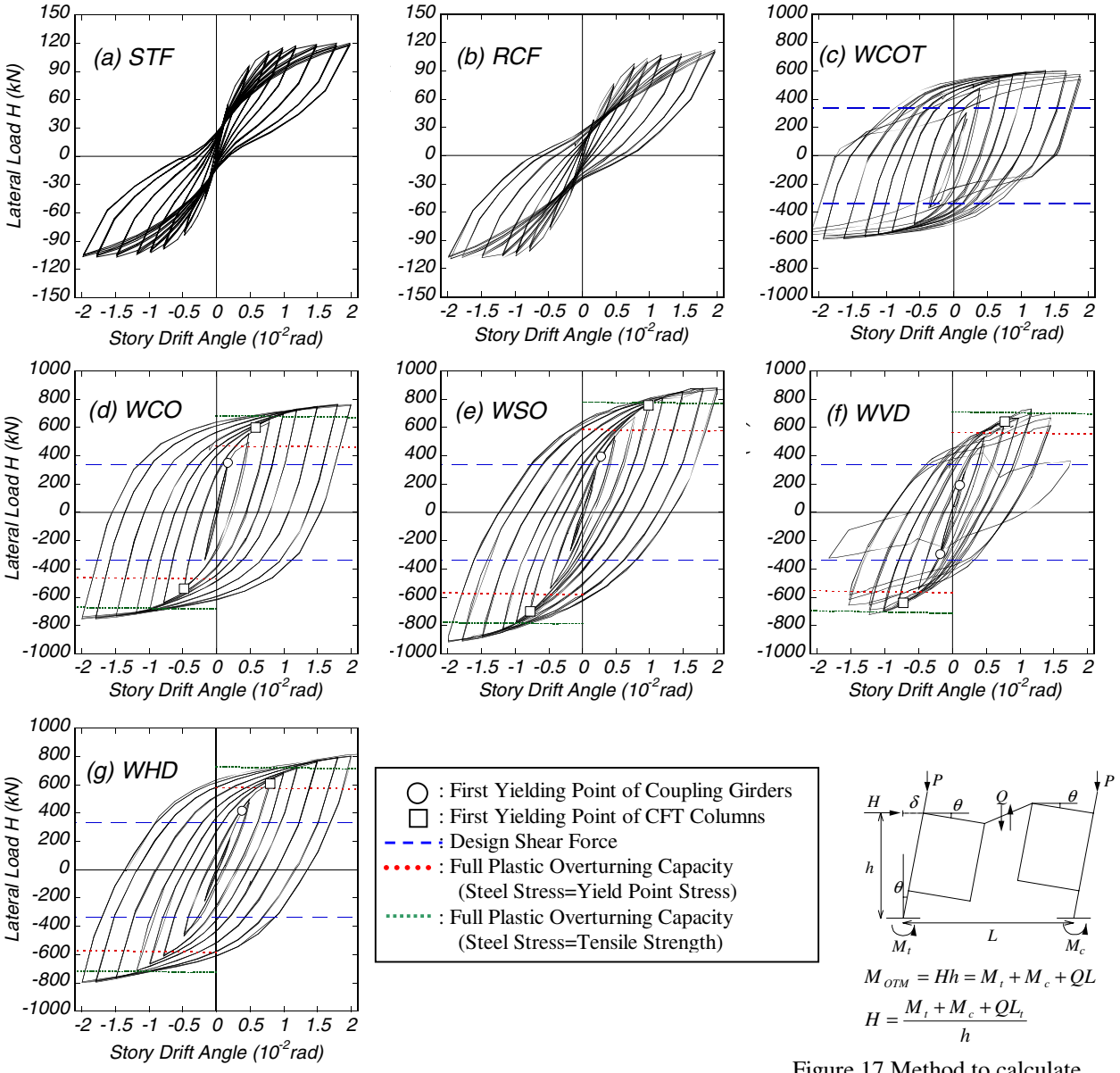

Figure 16 Experimental results of lateral load versus story drift angle relationships.

$$M_{OTM} = Hh = M_t + M_c + QL$$

$$H = \frac{M_t + M_c + QL_t}{h}$$

Figure 17 Method to calculate full plastic overturning moment capacity.

equation given in Figure 17, where M_t and M_c are full plastic moment capacities of the CFT columns in tension and compression sides, respe ctively, and Q is a shear capacity of the coupling girder. The thin and

thick dotted lines are calculated by assuming that the steel strength is taken as a yield point stress or tensile strength obtained from coupon tests, respectively. The experimental maximum overturning capacity of all the wall specimens is larger than that shown by thick dotted line which shows theoretical upper bound capacity. The reason for this phenomenon is considered that the shear capacity of the coupling girder is calculated by igno ri ng a contribution of flanges of H-shaped section so called as a frame action of the flanges.

RELATIONSHIPS BETWEEN MEMBER DEFORMATION ANGLE OF COUPLING GIRDERS AND STORY DRIFT ANGLE

Figure 18 shows relationships between member deformation angle of coupling girders and story drift angle. As can be seen in Figure 18, member deformation angles are three to five times of the story drift angles, which means that the coupling girder of each wall specimen yielded at early stage of the test, and behaved as the hysteretic damper. The relationships shown in Figure 18 have a common feature that they are composed of two parallel lines with steeper slope and many curves with gentle slope connecting two parallel lines. A number of groups of gentile slope curves correspond to a number of story drift amplitude in loading program shown in Figure 14. Gradients of two parallel lines shows ratio of the member deformation angle of coupling girder to the story drift angle which can be calculated based on a kinematics mode of collapse mechanism composed of rigid body, two plastic hinges in bottoms of edge columns and coupling girder yielded in shear behaving as pin connected rigid link. The curves connecting two parallel lines show relationships between the member deformation angle of coupling girder and story drift angle of the walls which behave in elastic and elastic-plastic manners before the collapse mechanism is fully developed. The gradient of these curves of each wall specimen depends on deformations of the wall panels and short edge columns connecting wall panels and foundation beam which are included only in story drift angle. Therefore, the ratio of the member deformation angle of coupling girder to the story drift angle is smaller than that in the kinematics mode of the collapse mechanism. It could be considered that a distance between the two parallel lines roughly corresponds to amount of shear deformations of the wall panels and short edge columns. Hereafter, the distance between the two parallel lines is referred to as "shear deformation" of wall specimens, even though it is not correct in the strict sense of the term.

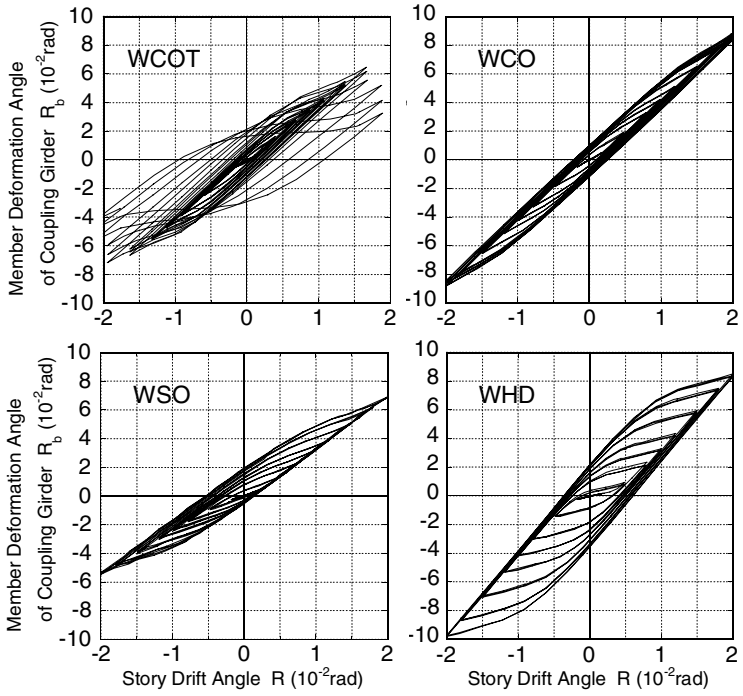

Figure 18 Experimental results of member deformation angle versus story drift angle relationships.

As shown in Figure 18, the shear deformations of WCO specimen are smaller than those of other wall specimens, because the wall panel of WCO specimen has the steel plate with stiffeners shown in Figure 9. A reason that the shear deformations of WCOT specimen having wall panels similar to those of WCO specimen are larger than those of WCO specimen especially in large story drift amplitude is due to the sliding shear slips at the bottoms of the tubed RC edge columns as described

before. The sliding shear slips introduce a pinched shape in hysteretic curves of WCOT specimen, because the sliding shear slips occur at some constant level of lateral force without any increments of the member deformation angle of the coupling girder as inferred from Figure 16(c). The less the shear deformation of the wall system are, the larger the member deformation angles of the coupling girder are. This results in an enhance of a function of the coupling girder as the hysteretic damper, if possible events such as a fatigue failure and cracks in welding portions of coupling girders are prevented by careful detailing of the coupling girders. It should be noted that the horizontal loads were applied in a manner which introduced the larger horizontal loads at the point where overturning collapse mechanism was fully developed than those in the wall systems in buildings at the base as expected from the results of the dynamic response analysis shown in Figure 7. In other words, it is expected that the actual hysteretic curves of the OTC wall systems would be more desirable shape such as those of WCO specimen shown in Figure 16(d). It is also expected that the problems of the fatigue failure and cracks in welding portions of coupling girders are not serious as far as the rolled H-shaped steel section is used as the coupling girders, since those possible events were not observed in any of the wall specimens which experienced large story drift angle up to 0.04-0.06h after cyclic loading tests shown in Figure 14.

OTHER DEFORMATIONS

The deformation characteristics of three wall specimens, WCO, WSO and WHD, which behaved in an expected manner to the OTC wall up to large story drift, are discussed in this section. Figures 19 and 20 show relationships between story drift angle and axial shortenings or rotational angles at second floor level (lateral loading point), respectively. These two kinds of deformations of the walls were obtained by measurements of axial shortenings in total height of both edge columns. The axial shortenings of the wall

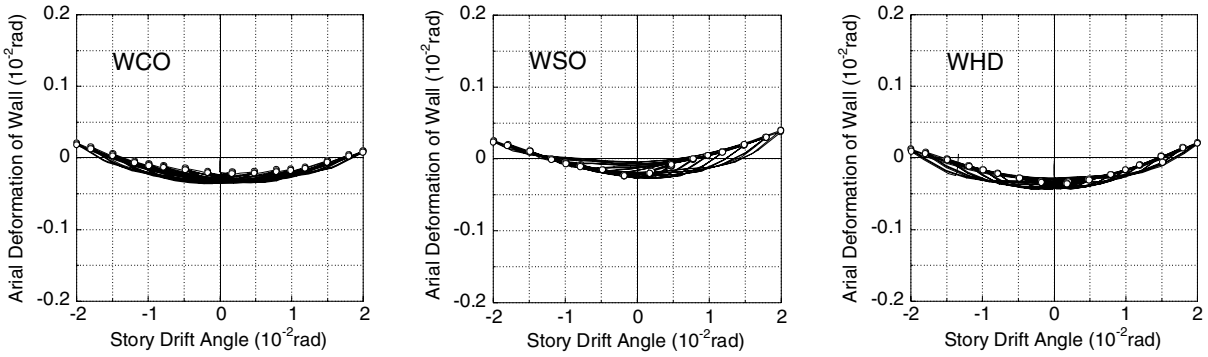

Figure 19 Experimental results of axial deformation of wall versus story drift angle relationships.

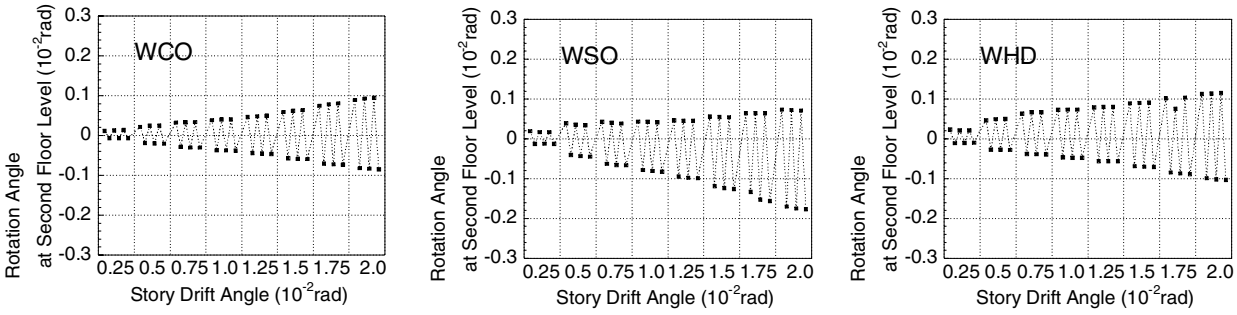

Figure 20 Experimental results of rotation angle of wall at second floor level versus story drift angle relationships.

specimens are defined as mean values of those of both edge columns, and the second floor rotation angles are obtained from differences of axial shortenings of the right and left edge columns divided by the

distance between both columns (span length). Figure 19 shows that axial shortening or elongations of the wall specimens are very small, which is an evidence of stable behavior of plastic hinges formed at the bottoms of edge columns. Figure 20 shows the second floor rotation angles at unloading points in each cycle, which are between 5 to 10 % of story drift angles and are almost negligible. This means that nodal points or beat-to-column connections are regarded to move only horizontal direction as moment resisting open frames are. This is an important feature of the OTC walls, since a complicated three-dimensional behavior of the dual system with the flexural yield type of cantilever structural walls, which always annoys structural engineers, is not introduced into the dual system with the OTC walls.

ANALYTICAL METHOD

In the analytical phase of this study, the computing program coded by Kawano (1998) was used. This analysis employs a finite element method using beam-column elements. Geometric nonlinearities are treated using an updated-Lagrangean formulation with a local coordinate axis for each element, which moves with the element within the global axis system. The element stiffness is evaluated by the Gaussian numerical integrals. The stiffness of a cross section is numerically integrated by dividing the section into a number of layers referred to as stress fibers. Fig ure 21 shows analytical models for the OTC walls, where the wall panels are replaced by two elastic braces for ECOT and WCO specimens having steel plates with stiffeners in the wall panels. On the other hand, the wall panels are replaces by many pin-connected diagonal plain concrete members, which are effective only in compression, for WSO and WHD sp ecimens, since separati ons between a steel fra mes and reinforced concrete panels were observed during the tests. The stress-strain models f or the concrete and the steel are shown in Figure 22 and Figure 23, respectively. The compr essive strength of concrete is taken as cylinder strengt h for that in the CFT columns, and 1.3 times of the cylind er strength for that in the tubed RC columns to take a confinement effect of the steel tube used for the specimen into consideration (Sun et al., 1998).

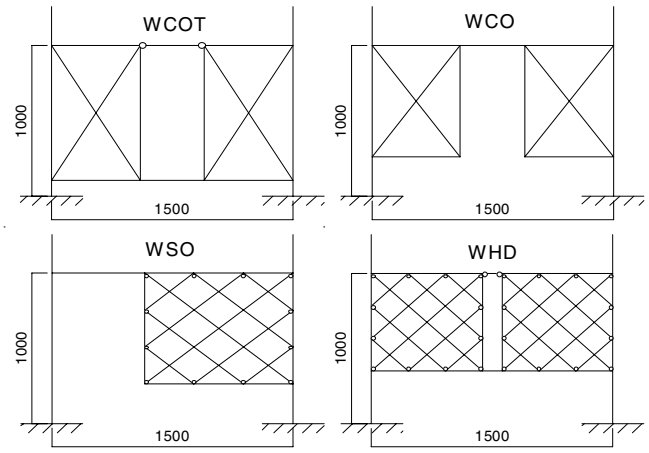

Figure 21 Analytical models for wall specimens.

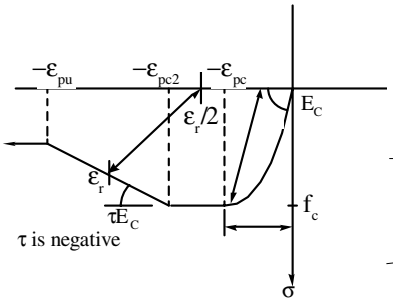

Figure 22 Stress-strain curve model for concrete.

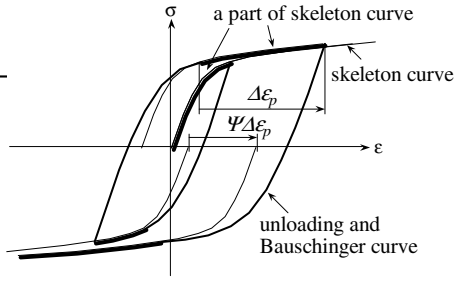

Figure 23 Stress-strain curve model for steel.

COMPARISONS BETWEEN ANALYTICAL AND EXPERIMENTAL RESULTS

The analytical results on lateral load – story drift angle relationships of the four wall specimens are shown in Figure 24. A reasonable agreement is o bserved between the experimental and the analytical results except for WCOT specimen. There is some discrepancy betwe en the analytical and experimental results of WCOT specimen at large story drift regions. The reason for this discrepancy is attributed to sliding shear slips occurred at the bottom s of the tubed RC e dge columns which are not considered in the

analysis. Other experimental results on deformations or strains, which are member deformation angles of the coupling girders, shear distorti ns of the wall panels and strains in concrete panels, are shown in Figures 25, 26 and 27, respectively. It is concluded t hat the analytical method utilizing the analytical models shown in Figure 15 can predict the experimental results very well.

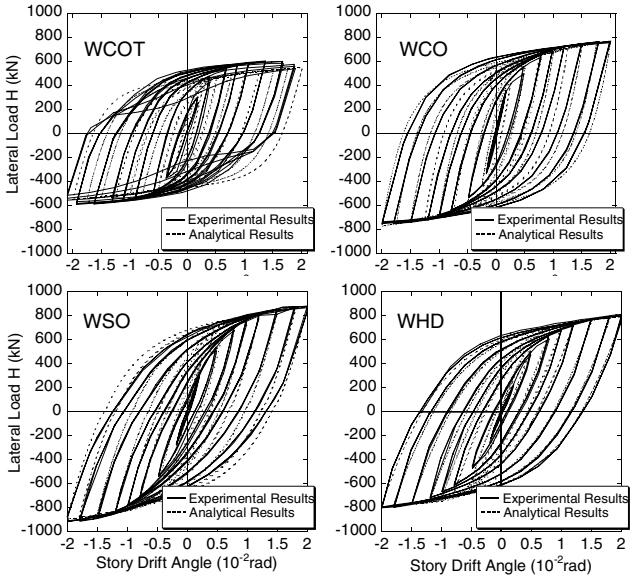

Figure 24 Comparisons between experimental and analytical results of lateral load versus story drift angle relationships.

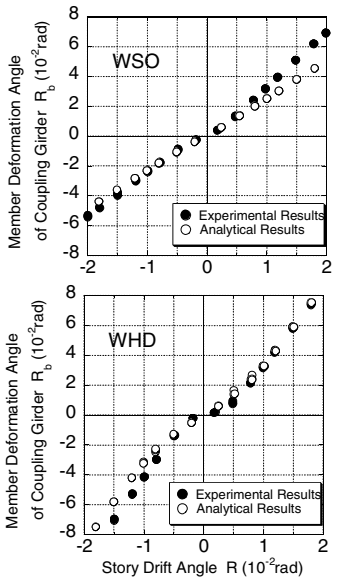

Figure 25 Comparisons between experimental and analytical results of member deformation angle of coupling girder versus story drift angle relationships.

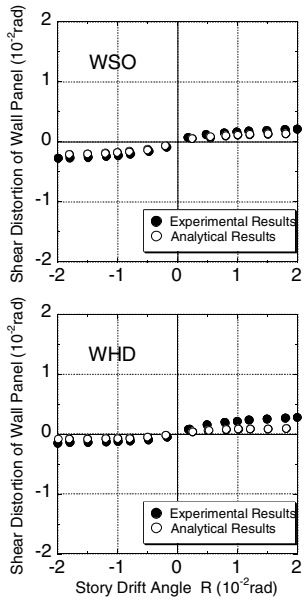

Figure 26 Comparisons between experimental and analytical results of shear distortion versus story drift angle relationships.

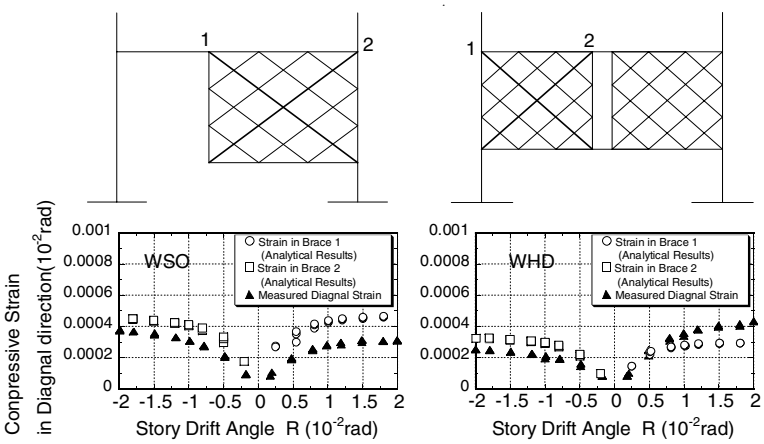

Figure 27 Comparisons between experimental and analytical results of strains in wall panel versus story drift angle relationships.

CONCLUSIONS

The following conclusions are reached on bases of the experimental study on the composite structural walls developing a new type of collapse mechanism generated by overturning moment.

(1) Four types of composite walls designed to be failed in overturning collapse mechanism were fabricated and tested under the cyclic lateral loading condition. Three of them behaved in a satisfactory manner as expected from a view point of the basic criteria, i.e. stiffness, strength, and energy absorption capacity. The other specimen behaved in a manner similar to that of three specimens described above, but finally failed in an undesirable and unexpected mechanism such as fractures of steel bars at story drift level larger than 0.015h. Indications of any kinds of shear failure were not observed in the plastic hinges developed at the bottoms of the concrete filled steel tubular columns. However, sliding shear slips were observed in the plastic hinges developed at the bottoms of the tubed RC columns at story drift level larger than 0.015h.

(2) The coupling girders in the wall specimens yielded at the small story drift, and absorbed a large amount of energy without a severe damage in appearance. It is concluded that the H-shaped steel coupling girders can take a role of the hysteretic damper.

(3) It was observed in the test of the two open frames that the reinforced concrete columns confined by the square steel tube behaved in a ductile and stable manners without damage to be repaired after a severe earthquake. There is no reason for avoiding column hinging during a severe earthquake from a view point of performance-based design philosophy, if the soft story mechanism is prevented by the structural walls.

(4) The behavior of the wall specimens can be predicted with a reasonable accuracy by the analytical method used in the analytical phase of this study.

ACKNOWLEDGEMENTS

The valuable contributions of Professor A. Kawano of Kyushu University to the analytical study and the contributions of a former graduate student T. Takahashi and an under graduate student M. Taguchi of Kyushu Unive rsity to the experimental study reported in this paper are greatly acknowledged.

REFERENCES

1. Architectural Institute of Japan (1990), *Design Guidelines for Earthquake Resistant Reinforced Concrete Building Based on Ultimate Strength Concept*, Nov. 1990 (in Japanese)

2. Bertero. V. V., Popov, E. P., Wang, T. Y., and Ballenas, J., (1977), "Seismic design implications of hysteretic behavior of reinforced concrete structural walls," 6th World Conference on Earthquake Engineering, New Delhi, Vol. 5, 1976: 159-165.

3. Paulay, T. and Priestley, M.J.N. (1992), "*Seismic design of reinforced concrete and masonry buildings,*" John Wiley & Sons, New York.

4. Hitaka, T. and Sakino, K., (2003), "Seismic performance of multi-story frames incorporating composite shear walls," Proceedings of the International Conference on Advances in Structures, Sydney, Australia, 22-25 June 2003: 1333-1338.

5. Tomii, M., Sakino, K. and Xiao, Y., (1987), "Ultimate moment of reinforced concrete short columns confined in steel tube," Proceedings of Pacific Conference on Earthquake Engineering, New Zealand, August 1987:1-14.

6. Kawano, A., Griffith, M.C., Joshi, H.R. and Warner, R.F., (1998), "Analysis of the behavior and collapse of concrete frames subjected to seismic ground motion," Department of Civil and Environmental Engineering, The University of Adelaide, Nov. 1998, Australia, Research Report No. R163.

7. Sun, Y.P., Sakino, K., Aklan, A. and Ikenono, Y., "Ultimate strength and deformability of RC columns retrofitted by square steel tube," Proceedings of the 2nd International RILEM/CSIRO/ACRA Conference, 1998: 619-632.